S. Cacciola, C.E.D. Riboldi, A. Croce
Monitoring Rotor Aerodynamic and Mass Imbalances Through a Self-Balancing Control
Journal of Physics: Conference Series, Vol. 1037, 2018, 032041 (11 pages)
doi:10.1088/1742-6596/1037/3/032041

Monitoring rotor aerodynamic and mass imbalances through a self-balancing control

IOP Conf. Series: Journal of Physics: Conf. Series **1037** (2018) 032041 doi:10.1088/1742-6596/1037/3/032041

Monitoring rotor aerodynamic and mass imbalances through a self-balancing control

S. Cacciola[1], C.E.D. Riboldi[1], A. Croce[1]

[1] Dipartimento di Scienze e Tecnologie Aerospaziali, Politecnico di Milano, Milano, Italy

E-mail: {stefano.cacciola, carlo.riboldi, alessandro.croce}@polimi.it

Abstract.

A typical concern in rotating systems is related to rotor imbalances, which result typically from pitch misalignment and unbalanced mass distribution. A novel control for simultaneously targeting mass and pitch imbalances on the rotor is presented. Additionally, a novel detection strategy is developed in order to detect the imbalance source out of the behavior of the control action. More in depth, since the control will generate an artificial aerodynamic imbalance which compensates the pre-existent aerodynamic and inertial ones, one can find and interpret the fingerprint of the imbalance source in the behavior of the balancing controller. A clear advantage of this approach is that the imbalance detection is performed while the control keeps the machine working within its operating limits reducing the down-time and unscheduled maintenance actions.

1. Introduction

Rotor imbalances is one of the major issues in rotating machinery, for they affect significantly the vibratory behavior of such machines.

In the case of large wind turbines, imbalances are typically caused by pitch misalignment, alteration of blade aerodynamic characteristics and unbalanced mass distribution.

Specifically, pitch misalignment may depend on incorrect blade mounting or on possible drifts of the pitch variation system. Mass imbalance may be due to asymmetric ice accretion, whereas the modification of blade aerodynamics is due to dirt and soiling.

For small and very small wind turbines, such as the models employed in wind tunnel experimentation, the problems related to imbalances are even more pronounced. In fact, due to the limited dimensions and weight, the rotor balancing are more sensible to manufacture errors, cable position and modification of the electronic and mechanical parts due to aging.

It is well known that, independently of the source, an imbalance will cause an abnormal increase of loading at the rotor frequency (1×Rev) in any fixed part of the turbine, e.g. tower, nacelle and bearings [1]. Following this concept, one may detect the presence of imbalances easily by analyzing 1×Rev harmonic in nodding, yawing moments or tower top accelerations. Once understood that a rotor is unbalanced, the turbine gets shut down and a maintenance action is scheduled [2]. In general, aerodynamic and mass imbalances have a similar impact on rotor loads and differentiating automatically between the two is a very difficult task, which requires more sophisticated approaches [3, 4, 5]. In case the sole pitch misalignment is of concern, the opportunity to cope with this issue using automatic control has gained the attention of researchers, as witnessed by some recent publications [6, 7, 8, 9, 10].

The scope of this paper is twofold. First, the formulation of the self-balancing control developed in [6] and [7] is extended in order to make it able to target not only pitch misalignment-induced but also mass imbalance-induced loads. In practice, the the self-balancing control will generate an artificial aerodynamic imbalance which compensates the inertial one, if present, and a pre-existent aerodynamic imbalance due to pitch misalignment or blade aerodynamic inequality. This way, the imbalance results automatically corrected and, in turn, the rotor balanced, without the need of any action by operators.

Second, a novel detection strategy is developed in order to detect imbalance source and severity out of the behavior of the control action. The basic idea of the new detection strategy is pretty intuitive. Clearly, the control, to counteract a sole pitch misalignment, needs to employ a constant balancing action. On the other hand, if also mass imbalance affects the rotor, the situation changes. In fact, since the inertial eccentricity generates some rotor-speed-dependent centrifugal forces, responsible for imbalance loading, the balancing control input results dependent on the machine operative condition. In other words, one can find and interpret the fingerprint of the imbalance source in the behavior of the balancing controller.

A clear advantage of this approach is that the imbalance detection is performed while the control keeps the machine working within its operating limits, reducing both the down-time losses and the unscheduled maintenance actions. It is therefore expected that such control may beneficially impact the cost of the energy, in terms of increasing capacity factor and decreasing of maintenance costs.

In this paper, we summarize briefly the self-balancing control algorithm and extend it so as to consider the possible presence of inertial imbalances. Finally, the detection strategy are detailed along with a selection of simulated results proving the effectiveness of the proposed procedure.

2. Method

2.1. Balancing control based on the Multiblade Multilag transformation

At first, consider the case of a pitch misaligned rotor operating in steady wind conditions. In such a regime, the out-of-plane blade loads, m_1, m_2 and m_3, result to be periodic with respect to the rotor azimuth ψ. The mean value of the three loads differ each other for significant biases, b_1, b_2 and b_3, caused by the pitch offset itself, in contrast with the balanced case where the loads oscillate around the same mean value. Accordingly, the blade moments could be expanded as

$$\begin{aligned} m_1(\psi) &= a_0 + b_1 + \sum_n a_{n_\mathrm{c}} \cos(n\psi_1) + a_{n_\mathrm{s}} \sin(n\psi_1) \\ m_2(\psi) &= a_0 + b_2 + \sum_n a_{n_\mathrm{c}} \cos(n\psi_2) + a_{n_\mathrm{s}} \sin(n\psi_2) \\ m_3(\psi) &= a_0 + b_3 + \sum_n a_{n_\mathrm{c}} \cos(n\psi_3) + a_{n_\mathrm{s}} \sin(n\psi_3), \end{aligned} \tag{1}$$

where ψ_i is the azimuth angle of the ith blade, such that $\psi_1 = \psi$, $\psi_2 = \psi + 2\pi/3$ and $\psi_3 = \psi + 4\pi/3$, and finally a_0 represents the constant, or $0\times$Rev, harmonic while a_{n_c} and a_{n_s} the cosine and sine amplitudes of the $n\times$Rev.

In order to simultaneously extract the $1\times$Rev and $2\times$Rev harmonic amplitudes, named respectively $\boldsymbol{a}_1 = \{a_{1_\mathrm{c}}, a_{1_\mathrm{s}}\}^T$ and $\boldsymbol{a}_2 = \{a_{2_\mathrm{c}}, a_{2_\mathrm{s}}\}^T$, and the biases of the three blades, $\boldsymbol{b} = \{b_1, b_2, b_3\}^T$ from blade moments, it is possible to employ an ad hoc transformation based on the Multiblade Multilag (MBML) concept, as reported in [6, 7]. The concept behind the MBML transformation is to exploit multiple samples, at different azimuthal lagged angles, of the multiple blade signals. The employed number of lags and the azimuthal sampling determine different transformations for different applications. In the particular case of pitch misalignment the transformation uses the three blade loads, collected in vector $\boldsymbol{m} = \{m_1, m_2, m_3\}$ at the

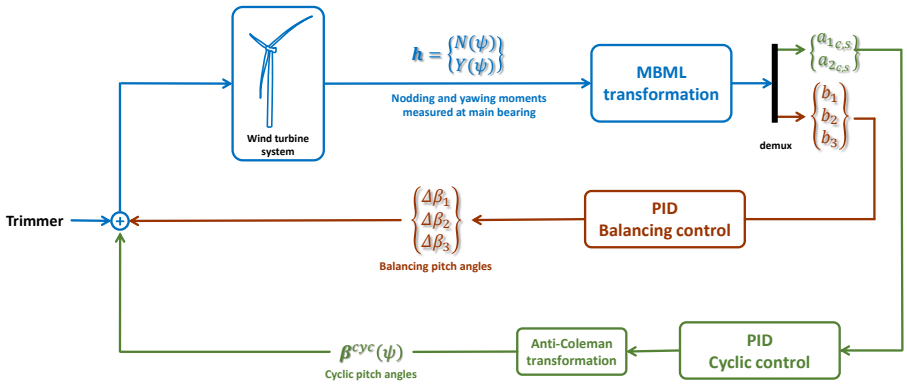

Figure 1. Control scheme.

current azimuth ψ, and at one lagged position $\psi - 2\pi/3$. The final MBML transformation aimed at extracting simultaneously the 1× and 2×Rev cyclic loads and the imbalanced induced loads (cf. [6, 7]) results to be

$$\begin{Bmatrix} a_0 \\ \boldsymbol{a}_1 \\ \boldsymbol{a}_2 \\ \boldsymbol{b} \end{Bmatrix}_{\mathrm{E}} = \begin{bmatrix} \boldsymbol{z} & \boldsymbol{z} \\ \boldsymbol{TC}(\psi + \pi/6) & \boldsymbol{TC}(\psi - 2/3\pi - \pi/6) \\ \boldsymbol{TC}(2(\psi - \pi/12) & \boldsymbol{TC}(2(\psi - 2/3\pi + \pi/12) \\ \boldsymbol{B} & \boldsymbol{B}^T \end{bmatrix} \begin{Bmatrix} \boldsymbol{m}(\psi) \\ \boldsymbol{m}(\psi - \dfrac{2\pi}{3}) \end{Bmatrix}, \tag{2}$$

where the subscript $(\cdot)_{\mathrm{E}}$ indicates the MBML estimated quantities, $\boldsymbol{z} = \{1/3, 1/3, 1/3\}$, $\boldsymbol{T} = \mathrm{diag}\{\tan(\pi/6), \tan(\pi/6)\}$, while

$$\boldsymbol{C}(\psi) = \frac{2}{3}\begin{bmatrix} \cos(\psi_1) & \cos(\psi_2) & \cos(\psi_3) \\ \sin(\psi_1) & \cos(\psi_2) & \sin(\psi_3) \end{bmatrix} \quad \text{and} \quad \boldsymbol{B} = \begin{bmatrix} 1/3 & 0 & -1/3 \\ -1/3 & 1/3 & 0 \\ 0 & -1/3 & 1/3 \end{bmatrix}. \tag{3}$$

It is possible to demonstrates the following properties of the estimated quantities:

$$\begin{aligned} a_{0E} &= a_0 + b_{\mathrm{coll}} + \mathscr{O}(3 \times \mathrm{Rev}) \\ \boldsymbol{a}_{1E} &= \boldsymbol{a}_+ \mathscr{O}(3 \times \mathrm{Rev}) \\ \boldsymbol{a}_{2E} &= \boldsymbol{a}_+ \mathscr{O}(3 \times \mathrm{Rev}) \\ b_{iE} &= b_i - b_{\mathrm{coll}}, \quad i = 1, \ldots, 3 \end{aligned}, \tag{4}$$

where $b_{\mathrm{coll}} = (b_1 + b_2 + b_3)/3$. Notice that this MBML transformation, similarly to the standard MB transformation, outputs the amplitudes of 1× and 2×Rev harmonics, polluted by a high frequency $\mathscr{O}$(3×Rev) disturbance, which will be eventually filtered. In addition to that, the MBML is able to return also the imbalance born loads, ready to be used by a suitable control. Hence, as easily foreseeable, the estimated values of $\boldsymbol{a}_1$, $\boldsymbol{a}_2$ and $\boldsymbol{b}$ can be used as feed-back measurement for an individual pitch control scheme aimed at targeting pitch misalignment induced loads $\boldsymbol{b}$ and simultaneously cyclic loads $\boldsymbol{a}_1$ and $\boldsymbol{a}_2$, through straightforward PIDs, as depicted in Fig. 1.

Before finalizing the mathematical treatment of this transformation, it is worthwhile to consider the case of mass imbalance. The presence of an eccentric mass entails a periodic loading at 1×Rev due to gravitational and centrifugal forces mainly on hub loads. For this reason, in

this work, we have developed another MBML transformation which makes use of the nodding and yawing moment instead of blade loads, in order to provide a controller able to compensate also for the mass imbalance.

To this end, the dual transformation can be derived recalling the relation between blade moments and hub loads, which is

$$\boldsymbol{m}(\psi) = [\mathbf{1} \quad \boldsymbol{Q}(\psi)] \left\{ \begin{array}{c} M_0(\psi) \\ \boldsymbol{h}(\psi) \end{array} \right\} \tag{5}$$

where

$$\mathbf{1} = \left[\begin{array}{c} 1 \\ 1 \\ 1 \end{array} \right], \quad \boldsymbol{Q}(\psi) = \left[\begin{array}{cc} \cos(\psi_1) & \sin(\psi_1) \\ \cos(\psi_2) & \sin(\psi_2) \\ \cos(\psi_3) & \sin(\psi_3) \end{array} \right] \quad \text{and} \quad \boldsymbol{h} = \left\{ \begin{array}{c} N(\psi) \\ Y(\psi) \end{array} \right\} \tag{6}$$

with $M_0 = 1/3(m_1 + m_2 + m_3)$ being the collective out-of-plane moment. Notice that, although both nodding and yawing measurements are usually available on standard machines, the collective moment is not directly measurable but only acquirable through blade loads. This said, let us proceed with the definition of the transformation assuming to have access to M_0. At the end of the treatment, the effects of the lack of such measure will be assessed.

To this end, inserting (5) in (2), one gets

$$\left\{ \begin{array}{c} a_0 \\ \boldsymbol{a}_1 \\ \boldsymbol{a}_2 \\ \boldsymbol{b} \end{array} \right\}_{\mathrm{E}} = \left[\begin{array}{cccc} \frac{1}{2} & \mathbf{0}^T & \frac{1}{2} & \mathbf{0}^T \\ \mathbf{0} & \boldsymbol{TC}(\psi + \frac{\pi}{6})\boldsymbol{Q}(\psi) & \mathbf{0} & \boldsymbol{TC}(\psi - \frac{2\pi}{3} - \frac{\pi}{6})\boldsymbol{Q}(\psi - \frac{2\pi}{3}) \\ \mathbf{0} & \boldsymbol{TC}(2(\psi - \frac{\pi}{12})\boldsymbol{Q}(\psi) & \mathbf{0} & \boldsymbol{TC}(2(\psi - \frac{2\pi}{3} + \frac{\pi}{12})\boldsymbol{Q}(\psi - \frac{2\pi}{3}) \\ \mathbf{0} & \boldsymbol{BQ}(\psi) & \mathbf{0} & \boldsymbol{B}^T\boldsymbol{Q}(\psi - \frac{2\pi}{3}) \end{array} \right] \left\{ \begin{array}{c} M_0(\psi) \\ \boldsymbol{h}(\psi) \\ M_0(\psi - \frac{2\pi}{3}) \\ \boldsymbol{h}(\psi - \frac{2\pi}{3}) \end{array} \right\}, \tag{7}$$

where $\mathbf{0}$ is a null column vector of suitable dimensions.

Clearly, from (7), the unmeasurable M_0 has only effect on the a_0 value, which is not relevant for control purposes, whereas both harmonic amplitude and biases depends only the nodding and yawing moment measured at current and lagged position. Therefore, one can get rid of a_0 and M_0, without affecting the estimation of biases and harmonic amplitudes.

Although one may imagine employing more sophisticated control laws (Optimal, Model Predictive, Receding Horizon Controls) we strongly believe that the real problem to face when it comes to considering imbalances is not simply related to the type of control but rather to the choice of feed-back measurements. In fact, correcting automatically a pitch misalignment implies an independent motion of the blades, a thing which is not typically included in standard controllers applying only collective and cyclic pitch settings. In effect, such a decentralized activity could lead to a control which does not assure the simultaneous reduction of loads on both blade and hub sides, as demonstrated in [11]. On the other hand, as demonstrated in the present work, the proper selection of feed-back quantities and the way they are computed through a MBML transformation makes it easier to synthesize the decentralized controller. Moreover, especially for wind energy applications, the PID-based controllers, when effective, are generally preferred, because of their simplicity, over more complex controller types which may require accurate knowledge of the machine and its subsystems, not always available.

2.2. Detection of aerodynamic a inertial imbalances from balancing control inputs

2.2.1. Mass imbalance model Consider an inertially imbalanced rotor whose eccentricity can be modeled as mass m located at a radial distance r from rotor center, at an azimuthal angle ψ_{m} measured from the reference rotor azimuth and at longitudinal distance d from the rotor disk. Moreover, consider one or more fixed frame load sensors placed in different positions along the shaft s_i. Two forces are associated to this mass, the relative weight mg, being g the gravity

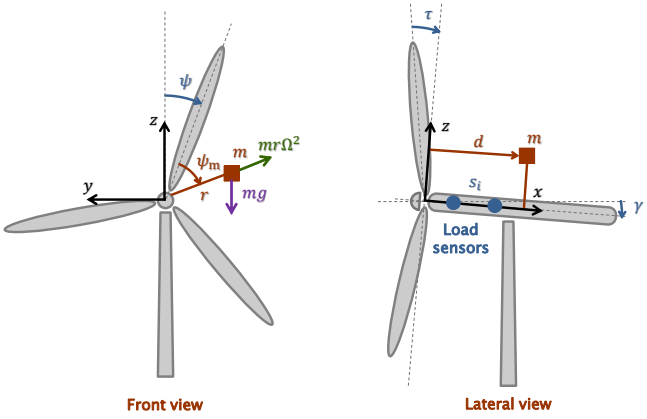

Figure 2. Representation of an eccentric mass modeling the inertial imbalance.

acceleration, and the centrifugal force $mr\Omega^2$, being Ω the rotor speed. Finally, rotor cone and uptilt angles are respectively named τ and γ. Turbine configuration is drawn in Fig. 2.

For rigid rotors, i.e. neglecting the dynamics of the coupled rotor-nacelle-tower system, the 1×Rev periodic excitation on nodding and yawing moment result

$$\begin{aligned} N_{1\times}|_{\text{mass imb.}} &= mr\left(g\sin(\gamma) + (s_i - d)\Omega^2\right)\cos(\psi + \psi_m) \\ Y_{1\times}|_{\text{mass imb.}} &= mr\left(g\sin(\gamma) + (s_i - d)\Omega^2\right)\sin(\psi + \psi_m) \end{aligned} \tag{8}$$

Collecting the characteristics of the eccentric mass (i.e. its value m, its static moment mr, its equivalent inertia mrd and its azimuthal position ψ_m), in a vector $\boldsymbol{q}^{(\text{mass imb})} = (m,\, mr,\, mrd,\, \psi_\text{m})^T$, one can express the 1×Rev nodding and yawing moment $\boldsymbol{h}_{1\times} = (N_{1\times},\, Y_{1\times})^T$ as a nonlinear function of $\boldsymbol{q}^{(\text{mass imb})}$, Ω and s_i as

$$\boldsymbol{h}_{1\times}|_{\text{mass imb.}} = \mathscr{M}(\boldsymbol{q}^{(\text{mass imb.})}, \Omega, s_i) \tag{9}$$

By looking at (8), it is clear that it is impossible to separate the effects of the mass m and of its radial position r as they appear in a product. For this reason, the estimation procedure will aim at estimation only the eccentric mass static moment mr instead of m and r separated.

2.2.2. Aerodynamic imbalance model In order to model the effect of pitch misalignment on hub loads, it is possible to recall the definition of cone coefficient, already introduced in [12, 13]. The cone coefficient C_m is a dimensionless measure of the out-of-plane blade bending moment as

$$C_m(\lambda, \beta, q) = \frac{M_0}{\left(\frac{1}{2}\rho V^2 R^3 \pi\right)}, \tag{10}$$

where λ is the Tip-Speed-Ratio (TSR), β the blade pitch angle, q the dynamic pressure, V the wind speed and R the rotor radius. Similarly to the power, torque or thrust coefficients, the cone coefficient is an aerodynamic characteristic of the rotor typically mapped as function of pitch, TSR and dynamic pressure.

Based on this definition, the ith blade moment m_i considering the possible effect of a pitch misalignment $\Delta\beta_i$ can be expressed as

$$m_i = \frac{1}{2}\rho V^2 R^3 \pi \left(C_{m_0} + C_{m_\beta}\Delta\beta_i\right), \tag{11}$$

where C_{m_0} is the cone coefficient value, independent from $\Delta\beta$, whereas C_{m_β} is the partial derivative of the C_m respect the blade pitch.

The loads of the misaligned blades induce the following nodding and yawing moments,

$$\begin{aligned}\left\{\begin{array}{c} N \\ Y \end{array}\right\} &= \left[\begin{array}{ccc} \cos\psi_1 & \cos\psi_2 & \cos\psi_3 \\ \sin\psi_1 & \sin\psi_2 & \sin\psi_3 \end{array}\right] \left\{\begin{array}{c} m_1 \\ m_2 \\ m_3 \end{array}\right\} = \\ &= \frac{1}{2}\rho V^2 R^3 \pi C_{m_\beta} \left[\begin{array}{cc} \cos\psi & -\sin\psi \\ \sin\psi & \cos\psi \end{array}\right] \left[\begin{array}{ccc} \cos(0) & \cos(2\pi/3) & \cos(4\pi/3) \\ \sin(0) & \sin(2\pi/3) & \sin(4\pi/3) \end{array}\right] \left\{\begin{array}{c} \Delta\beta_1 \\ \Delta\beta_2 \\ \Delta\beta_3 \end{array}\right\}\end{aligned} \tag{12}$$

So, finally, the 1×Rev nodding and yawing moment components induced by pitch misalignment can be computed as

$$\begin{array}{l} N_{1\times}|_{\text{pitch mis.}} = \frac{1}{2}\rho V^2 R^3 \pi C_{m_\beta} \left(\Delta\beta_c \cos\psi - \Delta\beta_s \sin\psi\right) \\ Y_{1\times}|_{\text{pitch mis.}} = \frac{1}{2}\rho V^2 R^3 \pi C_{m_\beta} \left(\Delta\beta_c \sin\psi + \Delta\beta_s \cos\psi\right) \end{array}, \tag{13}$$

where

$$\left\{\begin{array}{c} \Delta\beta_c \\ \Delta\beta_s \end{array}\right\} = \left[\begin{array}{ccc} \cos(0) & \cos(2\pi/3) & \cos(4\pi/3) \\ \sin(0) & \sin(2\pi/3) & \sin(4\pi/3) \end{array}\right] \left\{\begin{array}{c} \Delta\beta_1 \\ \Delta\beta_2 \\ \Delta\beta_3 \end{array}\right\} \tag{14}$$

Finally, the periodic loading due to pitch misalignment can be viewed as a non linear function of the pitch misalignment angles $\boldsymbol{\Delta\beta}^{(\text{pitch mis.})} = \{\Delta\beta_1, \Delta\beta_2\, \Delta\beta_3\}^T$, wind speed V and general wind turbine conditions, including air density, collective pitch angle, rotor speed, collected for simplicity in a vector $\boldsymbol{\alpha}$, as

$$\boldsymbol{h}_{1\times}|_{(\text{pitch mis.})} = \mathscr{A}(\boldsymbol{\Delta\beta}^{(\text{pitch mis.})}, V, \boldsymbol{\alpha}). \tag{15}$$

It is noteworthy that the balancing control actions $\boldsymbol{\Delta\beta}^{(ctrl)}$ act on loads equally to the pitch misalignment as

$$\boldsymbol{h}_{1\times}|_{\text{ctrl}} = \mathscr{A}(\boldsymbol{\Delta\beta}^{(\text{ctrl})}, V, \boldsymbol{\alpha}). \tag{16}$$

2.2.3. Estimation of imbalances The final nodding and yawing moments at 1×Rev results from the sum of three components induced by mass imbalance, pitch misalignment and that due to control action, as

$$\boldsymbol{h}_{1\times} = \boldsymbol{h}_{1\times}|_{\text{mass imb.}} + \boldsymbol{h}_{1\times}|_{\text{pitch miss.}} + \boldsymbol{h}_{1\times}|_{\text{ctrl}} \tag{17}$$

Clearly, the MBML-based control, described in Sec. 2.1, generates an artificial aerodynamic imbalance, whose effects are equal and opposite to the sum of those due to the inertial and aerodynamic imbalances capable of nullifying the total 1×Rev, $\boldsymbol{h}_{1\times}$.

As a remark, from (17), in the case of pure pitch misalignment the balancing control action will stay the same, independently of the change in the operative conditions of the turbine, e.g. wind speed, air density. This can be promptly observed by noting that both $\boldsymbol{\Delta\beta}^{(\text{PitchImb})}$ and $\boldsymbol{\Delta\beta}^{(\text{ctrl})}$ have effects on loading through the same function $\mathscr{A}$. Conversely, if a mass imbalance is present, the control action will change according to the rotor and wind speed.

In order to estimate the severity of the imbalance, i.e. the value of the pitch misalignment and the value and position of the eccentric mass, it is possible to fit model (17) to measurement data from an operating machine. To this end, consider K operative conditions, indexed with k, and W load sensors along the shaft, indexed with w. Define now the residue $\boldsymbol{\nu}_{k,r}$ between the output of model (17) and the actual measurement of $\boldsymbol{h}_{1\times}$, as

$$\boldsymbol{\nu}_{k,r} = \boldsymbol{h}_{1\times_{k,r}} - \Big(\mathscr{M}(\boldsymbol{q}^{(\text{mass imb.})}, \Omega_k, s_w) + \mathscr{A}(\boldsymbol{\Delta\beta}^{(\text{pitch mis.})}, V_k, \boldsymbol{\alpha}_k) + \mathscr{A}(\boldsymbol{\Delta\beta}^{(\text{ctrl})}{}_k, V_k, \boldsymbol{\alpha}_k)\Big) \tag{18}$$

Finally, the detection algorithm can be performed offline, after having collected a suitable amount of data, by the following minimization algorithm,

$$\boldsymbol{\theta} = \arg\left(\min\left(\sum_{k=1}^{K}\sum_{w=1}^{W}\boldsymbol{\nu}_{k,r}^{T}\boldsymbol{\nu}_{k,r}\right)\right) \tag{19}$$

where $\boldsymbol{\theta} = \{\boldsymbol{q}^{(\text{mass imb.})^T}, \boldsymbol{\Delta\beta}^{(\text{pitch mis.})}\}^T$.

3. Results

3.1. Balancing control performance

The MBML-based control was tested in a simulated environment through a high fidelity multibody model of a 3 MW wind turbine with a diameter of 92 m. The cut-in, rated and cut-out wind speeds are respectively 3, 12.5 and 25 m/s. The transition region II$\frac{1}{2}$ extends from 9 to 12.5 m/s. The aeroservoelastic wind turbine model is implemented in the finite element multibody code `Cp-Lambda` [14]. The model comprises flexible blades, tower and drive-train, implemented with geometrically exact nonlinear beam models, and compliant foundations. Moreover, the generator model considers mechanical losses. The aerodynamics is rendered through the blade element momentum theory (BEM) and includes corrections for hub/tip losses and unsteady behavior. Pitch and torque actuators are also included in the model as second and first order systems, respectively. The turbine model is controlled by an active pitch/torque speed-scheduled linear quadratic regulator (LQR) [15]. The total number of degrees of freedom is slightly more than 2500. Finally, the model is subjected to turbulent and non turbulent wind time histories generated by the code `TurbSim` [16].

Three different types of imbalance are considered. A pitch misalignment, with the pitch of blade #1 biased by an offset of 1 deg, with respect to the other two. An inertial imbalance with an eccentric mass attached to blade #1. Such mass is characterized by a static moment $mr = 4.2\text{E}3$ (equal to the 3% of the blade static moment) and is located at a distance from hub $d = -0.29$ m, resulting from the rotor cone of 2 deg, and at rotor azimuth $\psi_{\text{m}} = 0$. Finally, both aforementioned imbalance together.

At first, steady normal wind profile (NWP) conditions were considered at different winds from 3 to 23 m/s.

Figure 3 shows the yawing moment, left, and the blade pitch angles, right, at 6 m/s. In the upper plots it is analyzed the mass imbalance condition whereas, in the lower plots, the pitch misalignment case. The balancing control is engaged at rotor revolution 26 and targets the imbalance in a few rounds, nullifying the 1×Rev oscillation in the hub loads.

As a remark, the compensation is unable to recover the correct value of the collective pitch misalignment, as clear form Eq.(4) and previously demonstrated in [6, 7]. In fact, a generic pitch misalignment may entail also an alteration of the value of the collective pitch. Changing the collective pitch clearly does not produce any imbalance. Hence, the controller, while capable of targeting the difference between the pitch of each blade and the collective, cannot recover the original collective setting. Notice that this effect is common to any possible pitch misalignment detection and compensation strategy. To clarify this concept, consider the case of a sole pitch misalignment, see Fig. 3 bottom-right. Since only blade #1 is misaligned of 1 deg, the collective setting is biased by a value of 1/3 deg. The controller compensates the misalignment by pitching blade #1 to $-2/3$ deg and blade #2 and #3 to $+1/3$ deg. The effect is that the three blades have the very same pitch with a collective equal to 1/3 deg.

Figure 4 shows the change of the balancing pitch as a function of the wind speed, for the same three imbalance scenarios introduced above. Clearly, if only a pure pitch misalignment is present, the control action results independent from the wind speed (red solid curve). On the other hand,

a rather variable behavior of the balancing pitch is obtained for a inertially unbalanced rotor (blue dashed line). Finally, when mixing both imbalance sources the resulting mitigating pitch is the sum of those obtained previously (yellow dash-dotted curve). This demonstrates that the effects of inertial and aerodynamic imbalance can be superimposed.

It should be remarked that, from a monitoring standpoint, the effects shown in Fig. 4 suggest that one can detect whether an inertial imbalance is present by looking at the control action with respect to the wind speed: a constant behavior excludes the presence of mass imbalance.

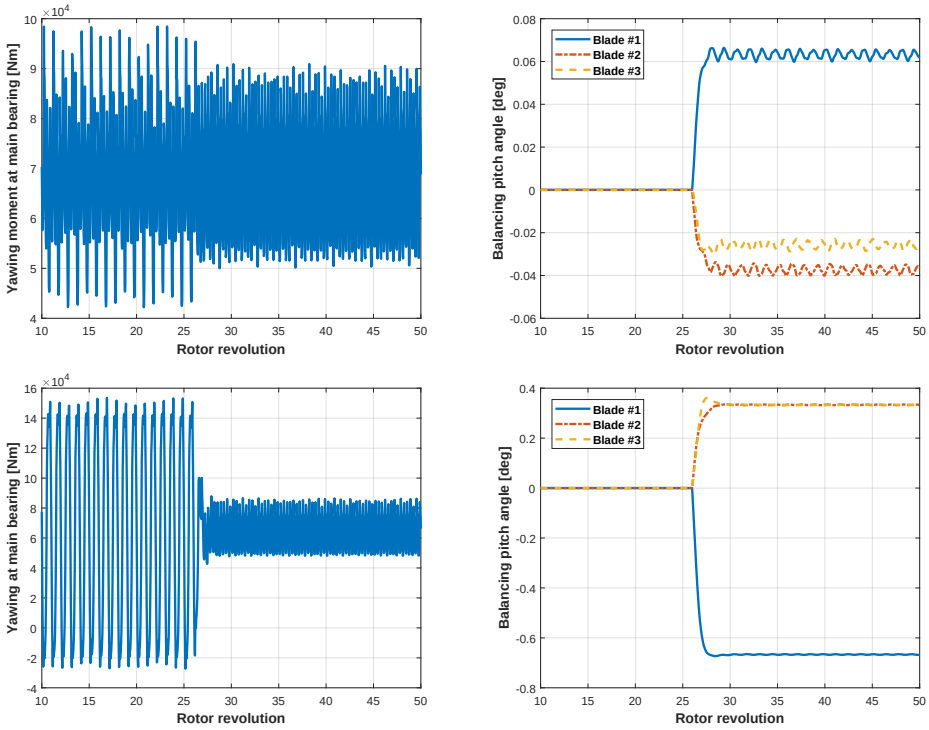

Figure 3. Yawing moment (left) and pitch angles (right). Top plots: mass imbalance; bottom plots: pitch misalignment. Comparison between uncontrolled and controlled behavior in NWP at 6 m/s. Balancing control is activated at revolution 26.

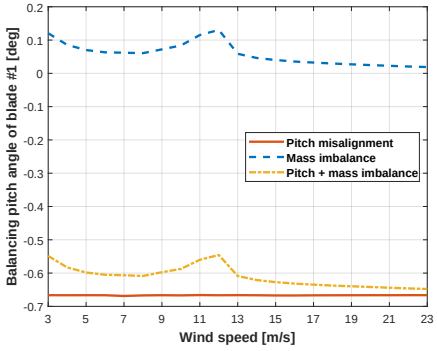

Figure 4. Balancing pitch angle of blade #1, $\Delta\beta_1$, as function of the wind speed.

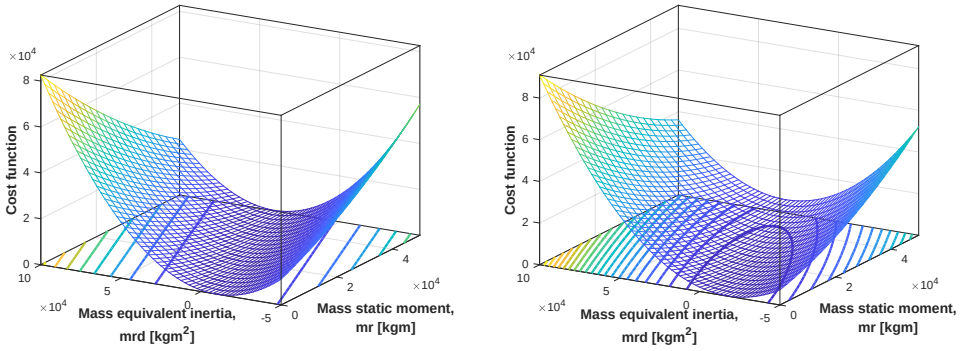

Figure 5. Check of observability of mass imbalance parameters. Cost function with one sensor (left) and with two sensors (right).

3.2. Detection of characteristics of mass and pitch imbalance

The detection strategy explained in Sec. 2.2 was then applied to the case of imbalance due to both aerodynamic and inertial causes. At first, the observability of the inertial and aerodynamic parameters to-be-estimated must be evaluated. In particular, issues were observed concerning the mass parameters. Figure 5 represents the cost function minimized in (19) for the cases in which only one sensor is used (left plot) and two sensors are deployed (right plot), as function of the mass static moment mr and equivalent inertia mrd. Clearly, from the left plot, the couple mr and mrd cannot be estimated together if only one sensor is used, as the cost function shape does not present a unique minimum, but rather a multiplicity of minima along a line. On the other hand, the usage of two sensors ensure the well-posedness of the problem as demonstrated by the shape of the cost function in the right plot.

Finally, Table 1 reports the estimation results obtained using two sensors.

Table 1. Estimates of the detection algorithm

		Real	Estimated
Pitch misalignment	$\Delta\beta_c$ [deg]	1	1.16
Pitch misalignment	$\Delta\beta_s$ [deg]	0	0.004
Mass static moment	mr [kg m]	4.14e+3	4.53e+3
Mass equivalent inertia	mrd [kg m^2]	-1.19e+4	-1.26e+3
Mass azimuthal position	ψ_{m}[deg]	0	-5.4

Clearly, the accuracy of the detection of pitch misalignment is very good, with an absolute error of 0.16 deg, whereas the estimates of mass imbalance result less accurate. In particular, the static moment and the azimuthal position of the eccentric mass can be observed with suitable precision, but the equivalent inertia presents significant errors, due to low observability.

Due to the low observability of the equivalent mass inertia mrd, one can hypothesize that $d = 0$ ($mrd = 0$) which corresponds to imposing the longitudinal position of the eccentric mass at the level of the rotor hub. Table 2 summarizes the obtained results. Improvement of the estimations of the pitch misalignment and of the mass azimuthal position is achieved at the price of a reduction of the accuracy in the estimation of the mass static moment mr.

Table 2. Estimates of the detection algorithm

	Real	Estimated	
Pitch misalignment	$\Delta\beta_c$ [deg]	1	1.0460
Pitch misalignment	$\Delta\beta_s$ [deg]	0	0.002
Mass static moment	mr [kg m]	4.14e+03	5.9e+03
Mass azimuthal position [deg]	0	-1.1	

4. Conclusions and outlook

In this paper a detection algorithm for mass imbalance and pitch misalignment is developed. The approach is based on the use of self balancing control able to target both kinds of imbalances. Before a possible real field application, a thorough experimental validation of the proposed methodology through a wind tunnel campaign is necessary. Such activity is underway. In the meanwhile, very promising results have been obtained in a virtual but realistic environment.

Based on the results the following conclusions can be argued.

- The self balancing control is able to effectively compensate for both aerodynamic and inertial imbalances without alterations to the control law and its tuning.
- The controller does not show any critical behavior and it is very effective in reducing imbalance born loads, which are annihilated in a matter of a few rotor revolutions.
- A detection algorithm can be designed capable of simultaneously estimating aerodynamic and inertial imbalance characteristics without impacting on the operative time of the machine. In particular, load and pitch measurements are collected while the balancing control is activated and is maintaining the turbine balanced and within its safe envelope.
- By studying only the behavior of the control inputs (i.e. balancing pitch angles) with respect to the wind speed, it is already possible to check whether the turbine is balanced or not and what the source of imbalance (aerodynamic or inertial) is, because the pitch misalignment is associated to a balancing control action constant with respect to the wind speed.

References

[1] Hameed Z, Hong Y, Cho Y, Ahn S and Song C 2009 Condition monitoring and fault detection of wind turbines and related algorithms: A review *Renew. Sust. Energ. Rev.***13**:1–39
[2] Kusiak A and Verma A 2011 A data-driven approach for monitoring blade pitch faults in wind turbines *IEEE Trans. Sustain. Energy***1** 87–96
[3] Cacciola S, Munduate Agud I and Bottasso CL 2016 Detection of rotor imbalance, including root cause, severity and location *J. Phys. Conf. Ser.* **753**(7):072003
[4] Kusnick J, Adams DE and Griffith DT 2015 Wind turbine rotor imbalance detection using nacelle and blade measurements *Wind Energy* **18**:267-276
[5] Kandukuri ST, Robbersmyr KG and Karimi HR 2014 Simultaneous estimation of mass and aerodynamic rotor imbalances for wind turbines *R. J. Math. Industry* **4**(1):1–19
[6] Cacciola S, Riboldi CED and Croce A 2017 A new decentralized pitch control scheme for wind turbines *IFAC-PapersOnLine* **50**(1):9908–9913.
[7] Cacciola S and Riboldi CED 2017 Equalizing aerodynamic blade loads through individual pitch control via multiblade multilag transformation *J. Sol. Energy Eng.* **139**(6):061008.
[8] Bertelè M, Bottasso CL, Cacciola S and Domestici M 2017 Automatic track and balance of wind turbine rotors *1st World Congress on Condition Monitoring*
[9] Petrović V, Jelavić M and Baotić M 2015 Advanced control algorithms for reduction of wind turbine structural load *Renew. Energ.* **76**:418–431
[10] Van Engelen TG and Kanev S 2009 Exploring the Limits in Individual Pitch Control *European Wind Energy Conference* (EWEC 2009)

[11] Bottasso CL, Croce A, Riboldi CED and Nam Y 2013, Multi-layer control architecture for the reduction of deterministic and non-deterministic loads on wind turbines *Renew. Energ.* **51**:159–169.
[12] Bottasso CL, Cacciola S and Schreiber J 2018, Local wind speed estimation, with application to wake impingement detection *Renew. Energ.***116**:155–168.
[13] Bottasso CL, Cacciola S and Schreiber J 2015, A wake detector for wind farm control *J. Phys. Conf. Ser.* **625**(1):012007.
[14] Bottasso CL and Croce A 2006-2018, Cp-Lambda User's manual.
[15] Bottasso CL, Croce A, Nam Y and Riboldi CED 2012, Power curve tracking in the presence of a tip speed constraint, *Renew. Energ.***40**(1), 1–12.
[16] Jonkman BJ and Kilcher, L 2012, TurbSim user's guide: version 1.06.00, NREL Technical report.